

# CALIBRATION OF DISCRETE ELEMENT SIMULATION PARAMETERS FOR BUCKWHEAT SEEDS

## 荞麦种子离散元仿真参数标定

Yulong CUI<sup>1,2)</sup>, Shaobo YE<sup>1,2)</sup>, Shuai FENG<sup>1,2)</sup>, Decong ZHENG<sup>1,2)</sup>

<sup>1)</sup> College of Agricultural Engineering, Shanxi Agricultural University, Taigu 030801, China;

<sup>2)</sup> Dryland Farm Machinery Key Technology and Equipment Key Laboratory of Shanxi Province, Taigu 030801, China

Corresponding author: Shaobo Ye

Tel: +86-152-3435-5087; E-mail: yes@sxau.edu.cn

DOI: <https://doi.org/10.35633/inmateh-75-09>

**Keywords:** Buckwheat; Parametric calibration; Discrete element; Angle of repose

### ABSTRACT

To address the challenge of parameter accuracy in discrete element method (DEM) simulations of buckwheat seeds within a seed metering device, this study characterized the physical properties of buckwheat seeds and subsequently calibrated the simulation model parameters. Initially, physical experiments were conducted to determine the triaxial dimensions, angle of repose, and static friction coefficients of buckwheat seeds against stainless steel surfaces. A three-dimensional model of the buckwheat seeds was then generated using Inventor and it was imported into EDEM to simulate the seed stacking process, with the angle of repose quantified via image processing techniques. Employing a Plackett-Burman design, initial parameters were screened, identifying the static friction coefficient between buckwheat seeds, the rolling friction coefficient between buckwheat seeds, and the static friction coefficient between buckwheat seeds and stainless steel as significant factors influencing the angle of repose. The optimal range for these significant parameters was determined through a steepest ascent experiment, and a second-order regression model was developed using Box-Behnken experimental results to optimize the angle of repose and the identified parameters. The optimized parameter set comprised a static friction coefficient between buckwheat seeds and stainless steel of 0.448, a rolling friction coefficient between buckwheat seeds of 0.038, and a static friction coefficient between buckwheat seeds of 0.372. Validation through both simulations and physical experiments revealed a relative error of 1.08%, confirming the reliability of the calibrated parameters for simulating buckwheat seed sowing machinery.

### 摘要

针对荞麦种子在排种器中进行离散元排种仿真模拟试验缺乏准确参数的问题,本研究对荞麦种子进行物性参数测定及仿真模型参数标定。首先,通过物理试验测定荞麦种子的三轴尺寸,休止角以及荞麦种子与不锈钢板间静摩擦系数。其次,运用 Inventor 绘制荞麦种子的三维模型,并导入到 EDEM 中建立荞麦离散元模型,来模拟荞麦种子的堆积过程,通过图像处理技术,获得准确的休止角。通过 Plackett-Burman 试验对初始参数进行筛选,得出荞麦间静摩擦系数、荞麦间滚动摩擦系数、荞麦-不锈钢之间的静摩擦系数对颗粒堆休止角影响显著。最后在最陡爬坡试验确定显著性参数最优值区间的基础上,根据 Box-Behnken 试验结果建立了休止角与显著性参数的二阶回归模型并对其进行优化,得到显著性参数的最佳组合。通过试验得出荞麦-不锈钢静摩擦系数为 0.448、荞麦间滚动摩擦系数为 0.038、荞麦间静摩擦系数为 0.372。通过仿真与物理试验对比验证,得到二者相对误差为 1.08%,标定参数可为荞麦播种机械仿真提供数据依据。

### INTRODUCTORY

Buckwheat is one of the small grains native to China, planted area of about 850,000 hm<sup>2</sup>, accounting for approximately one-third of the world's planted area. The average annual production is about 980,000 tons, ranking second globally (Wu L.G. et al., 2018). Buckwheat is valued for its unique functional components and high nutritional value, attracting increasing global attention. However, the level of mechanization in buckwheat sowing remains relatively low worldwide. In China's alpine and hilly regions, where buckwheat planting is extensive, mechanized harvesting is limited. Available models are scarce, and harvest quality is poor. Even in northern regions with higher mechanization levels, temporary modifications of other crop sowing machines are commonly used. These adaptations complicate interactions between seeds, seed dischargers, and machine components. Analysis using the discrete element method (DEM) allows for a detailed understanding of these interactions and facilitates the design and optimization of related equipment and process parameters (Zeng Z.W. et al., 2021).

Previous studies have calibrated DEM parameters for materials such as coal dust, cereal seeds, corn, potatoes, and garlic. *Zhang Rui et al., (2017)*, calibrated the contact parameters of sand and soil using standard and non-standard ball methods, and investigated whether different quality of sand and soil with different calibration methods would affect the results of stacking angle as well as the contact parameters. *Li Yong Xiang and others, (2019)*, simplified irregularly shaped wheat flour particles into soft spherical ones and scaled them, selected the “Hertz - Mindlin with JKR” contact model, and used the angle of repose to calibrate the contact parameters. *Wang Chengjun et al., (2012)*, determined the elastic properties of wheat and investigated the effects of collision material, material thickness, drop height and wheat moisture content on the coefficient of recovery of wheat, and determined the significance ranking of the effects of each factor on the coefficient of recovery of wheat for Q235 collision material. *Wu Jia Sheng et al., (2019)*, used the cylinder stacking method with EDEM simulation and combined with image processing technology to determine the stacking angle of forenut seeds, and calibrated the physical parameters of forenut seeds based on the response surface optimization method, *Liu Wen Zheng et al., (2018)*, optimized and calibrated potato parameters by combining physical and simulation tests. *González-Montellano et al., (2012)* studied maize and olive and obtained large CV (coefficient of variation) values for seeds at different collision velocities by means of a collision recovery test, which showed that in most cases the CV values were determined by the nature of the seeds themselves. In summary, it can be seen that most of the discrete element simulation calibration are powder, corn, seeds and large objects, and there is little content on the determination and calibration of discrete element simulation parameters of buckwheat grains.

This study combines physical and simulation tests to calibrate nine parameters for buckwheat grains. Physical test values were used as input ranges for Plackett-Burman, steepest climb, and Box-Behnken experiments. The results provide data support for future DEM simulations of buckwheat sowing machinery, enhancing simulation accuracy.

## MATERIALS AND METHODS

### **Static friction angle measurement test**

The static friction coefficient of buckwheat seeds represents the maximum static friction force divided by the normal force during contact. Seed surface roughness primarily determines this coefficient—greater roughness increases the coefficient and reduces seed movement tendency. The test apparatus is shown in Fig. 1. The oblique plane method was used to measure the static friction coefficient. The angle  $\theta$  was gradually increased until the seeds began to slide, at which point  $\theta$  was recorded.

The static friction coefficient  $\mu$  was calculated using Eq. 1 (*Li et al., 2023*).

$$\mu = \frac{f}{N} = \frac{mg\sin\theta}{mg\cos\theta} = \tan\theta \quad (1)$$

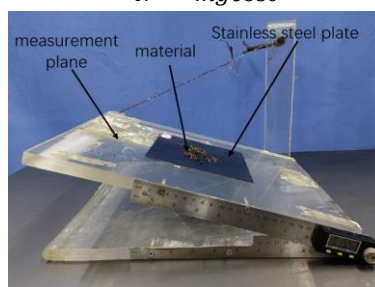


**Fig. 1 - Static friction measurement**

Based on the measured data, the angle of static friction between the buckwheat seeds and the stainless steel plate can be derived, and the static friction factor was calculated as 0.275.

### **Stacking Experiment**

The methods of angle of repose measurement include gravitational equilibrium method and internal collapse method. Based on the experimental conditions of our institute, the funnel method was adopted to measure the angle of repose. The funnel apparatus is illustrated in Fig.2, with a large diameter ( $a_1$ ) of 140 mm, a small diameter ( $a_2$ ) of 25 mm, and a height ( $h_1$ ) of 170 mm. The height of the funnel above the platform ( $h_2$ ) is 100 mm, and the diameter of the frustum ( $a_3$ ) is 100 mm. During the experiment, the distance between the bottom of the funnel and the frustum below ( $h_3$ ) was adjusted and buckwheat seeds were uniformly added

into the funnel at a constant rate. The seeds gradually formed a conical pile, with the angle between the slope of the conical pile and the plane of the frustum representing the angle of repose ( $\theta$ ), as shown in Fig.3.

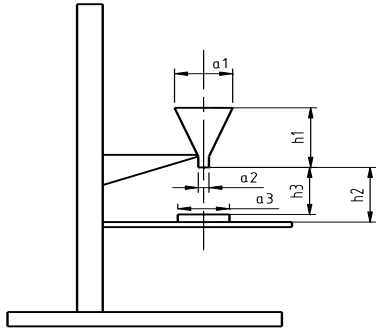


Fig. 2 - Schematic diagram of the funnel device



Fig. 3 - Buckwheat seed pile

In order to reduce human error in measurement, the computer image processing method Matlab is used here for image processing of buckwheat rest angle. As shown in Fig.4. First use the camera perpendicular to the side of the buckwheat pile to take a picture, to obtain the original image, as shown in Fig.4 (a).

The image is converted into a gray-scale image by Matlab processing as shown in Fig.4 (b), and then the image is binarized to obtain the binarized image, followed by extracting the curve data in the picture to obtain the boundary as shown in Fig.4 (c).

Subsequently the calibration between the picture and the curve is performed to obtain the unprocessed scatter plot. The scatter points are converted into useful curves and the scanned curves are shown in Fig.4 (d). Finally, the extracted data were fitted and the fitted curve was obtained as shown in Fig.4 (e). For each experiment, the repose angle of the buckwheat pile was measured in four directions: front, back, left, and right. The experiment was repeated twice to obtain an average value. The calculated repose angle  $\alpha$  for the buckwheat in the actual experiment was found to be  $27.65^\circ$ .

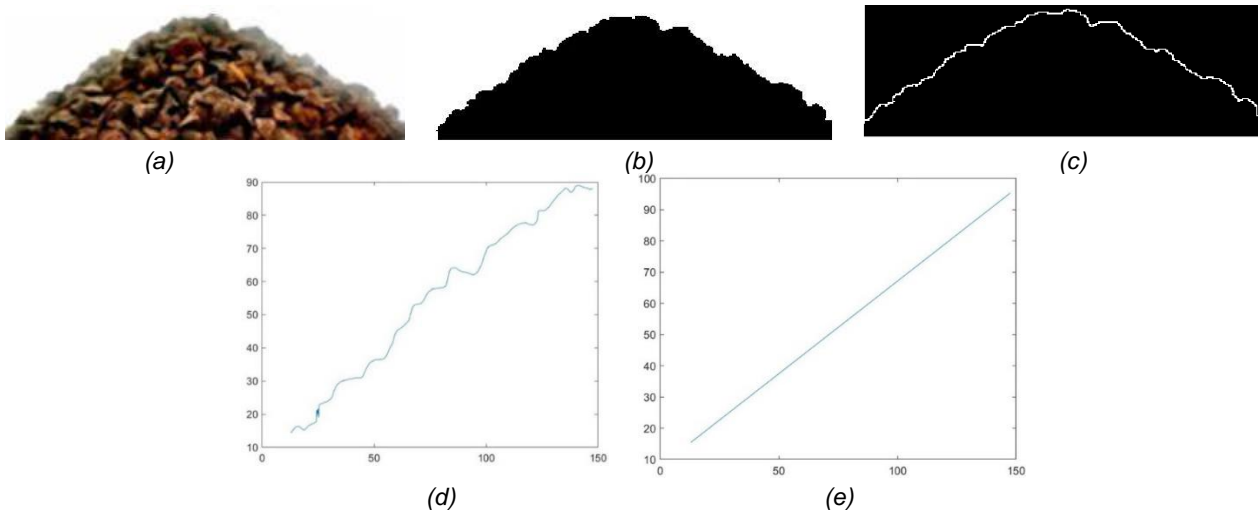


Fig. 4 - Angle of repose image processing

**Establishment of discrete elemental model and parameter calibration of buckwheat**

The discrete element model needs to roughly match the appearance of the actual object. In the discrete element simulation parameter settings, different input values give different results. Therefore, the physical test values are used as a target for the optimization of individual contact parameters (Xu B et al., 2021).

**Model building**

The three-axis dimensions of buckwheat were determined using a calliper, with the measurement results being presented in Table 1. This experiment focused on laboratory-cultivated bitter buckwheat and measurements were taken ten times to calculate the average value. Then, Inventor was used to draw the three-dimensional model of buckwheat, which was saved in STL format and imported into EDEM. Relevant literature shows that for the simulation modeling, smaller shape errors have less impact on the simulation results, and smaller errors between the size and shape of the actual particles and the discrete element model can be allowed. Therefore, the measured and statistical buckwheat shape dimensions were filled as shown in Fig. 5.

Table 1

Buckwheat triaxial size

	Length	Width	Height
maximum values /mm	6.15	4.92	4.58
average value /mm	6.01	4.13	4.09
minimum value /mm	5.84	4.02	3.96

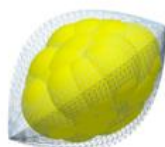


Fig. 5 - Discrete metamodel of buckwheat

**Modeling of the funnel**

The material chosen for the funnel is Q235 to model the discrete element of the funnel, where the diameter of the large end of the funnel is 140 mm, the diameter of the small end is 25 mm, and the height of the funnel is 170 mm. There is also a circular table with a diameter of 100 mm and a height of 7 mm (Chen G et al., 2024).

**Formation of particle stacks**

After the funnel model was established, it was imported into EDEM, and the dynamic particle generation method was used to establish a particle plane at the upper end of the funnel, the buckwheat seeds were discharged from the buckwheat grain container at a consistent rate, and eventually the grains would form a stable conical particle pile on the circular table. The whole process of seed grain formation is shown in Fig.6 (Lei et al., 2023).

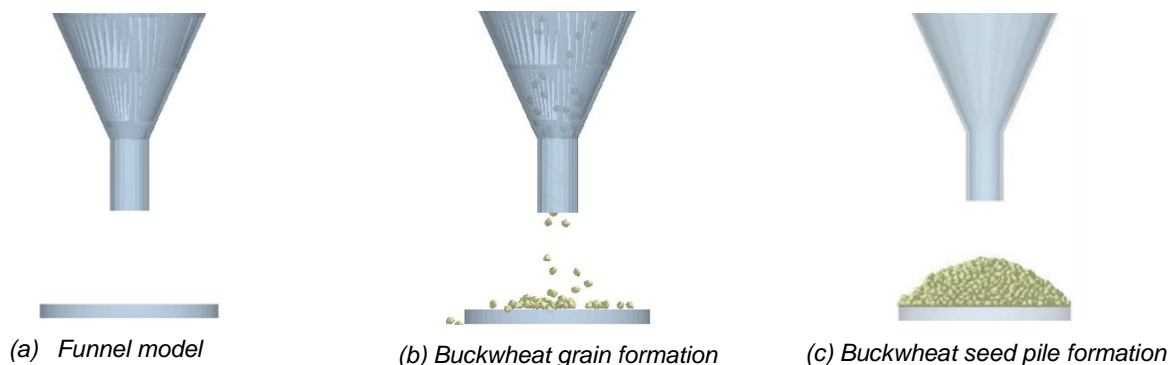


Fig. 6 - Simulated formation process of buckwheat kernels

**Simulation model parameter calibration test**

● **Plackett-Burman test**

Design-Expert software was applied to design the Plackett-Burman test, using the angle of repose of buckwheat seed drop test as the response value, and the simulation parameters with significant influence on the response value were screened out. It was combined with the previous physical tests and related literature to determine the individual simulation parameters in this study. The collision recovery coefficient for buckwheat ranges from 0.2 to 0.5, while the static friction coefficient is between 0.3 and 0.61. The rolling friction coefficient for buckwheat falls within 0.01 to 0.1. In interactions between buckwheat and stainless steel, the collision recovery coefficient is observed to be between 0.1 and 0.508, the static friction coefficient ranges from 0.2 to 0.7, and the dynamic friction coefficient is between 0.043 and 0.1. Simulation experiments were conducted to optimize nine parameters labelled A-I, selecting the upper and lower limits of two values to establish high and low levels, resulting in a total of 12 test groups, as detailed in Table 2 (Rittisak et al., 2023; Xu et al., 2023).

Table 2

Buckwheat simulation parameters

Symbol	Parameters	Levels	
		-1	+1
A	Buckwheat Intercollision Recovery Coefficient	0.2	0.5
B	Coefficient of static friction between buckwheat seeds	0.3	0.61
C	Coefficient of rolling friction between buckwheat seeds	0.01	0.1
D	Buckwheat seeds-stainless steel dynamic collision recovery coefficient	0.1	0.508
E	Buckwheat seeds-stainless steel coefficient of static and dynamic friction	0.2	0.7
F	Buckwheat seeds-stainless steel coefficient of kinetic friction	0.043	0.1
G	Buckwheat Poisson's ratio	0.3	0.5
H	Buckwheat density	1034	1250
J	Buckwheat shear modulus	1E+06	3.43E+06

- **Plackett-Burman experimental design**

Utilizing the Plackett-Burman design, the fundamental contact parameters influencing the buckwheat seed drop test as a variable factor were assessed, with each test yielding an average angle of repose of approximately 2. The experimental findings are presented in Table 3.

Table 3

Plackett-Burman experimental design

Test No.	A	B	C	D	E	F	G	H	J	Angle of repose / (°)
1	0.2	0.61	0.1	0.508	0.2	0.043	0.3	1250	1E+06	21.67
2	0.2	0.61	0.1	0.1	0.7	0.1	0.5	1034	1E+06	38.62
3	0.2	0.3	0.01	0.508	0.2	0.1	0.5	1034	3.43E+06	12.94
4	0.5	0.61	0.01	0.508	0.7	0.1	0.3	1034	1E+06	26.42
5	0.2	0.61	0.01	0.508	0.7	0.043	0.5	1250	3.43E+06	28.02
6	0.2	0.3	0.01	0.1	0.2	0.043	0.3	1034	1E+06	11.63
7	0.5	0.3	0.01	0.1	0.7	0.043	0.5	1250	1E+06	20.36
8	0.2	0.3	0.1	0.1	0.7	0.1	0.3	1250	3.43E+06	29.99
9	0.5	0.61	0.01	0.1	0.2	0.1	0.3	1250	3.43E+06	14.90
10	0.5	0.3	0.1	0.508	0.2	0.1	0.5	1250	1E+06	15.88
11	0.5	0.3	0.1	0.508	0.7	0.043	0.3	1034	3.43E+06	31.80
12	0.5	0.61	0.1	0.1	0.2	0.043	0.5	1034	3.43E+06	24.11

Analysis of variance was performed on the test data and the results of the Plackett-Burman test were used to identify significant effects using the Lenth method, which yielded a half-normal probability effects plot for the standardized effects of the factors as shown in Fig.7 (a) as well as a Pareto chart for the standardized effects of the factors as shown in Fig.7 (b). As can be seen from Fig.7 (a), the standardized effect points of factors B, C and E are farther away from the fitted line, so they are significant factors ( $P < 0.05$ ), that is, the significant factors affecting the angle of repose are the coefficient of static friction between buckwheat seeds, the coefficient of rolling friction between buckwheat seeds, the coefficient of static friction between buckwheat seeds - stainless steel, and the standardized effect points of the other factors are smaller. The Pareto chart of standardized effects, shown in Fig.7 (b), further determines the magnitude and significance of the effect, factors B, C, and E exceeded the t-value as a significant factor.

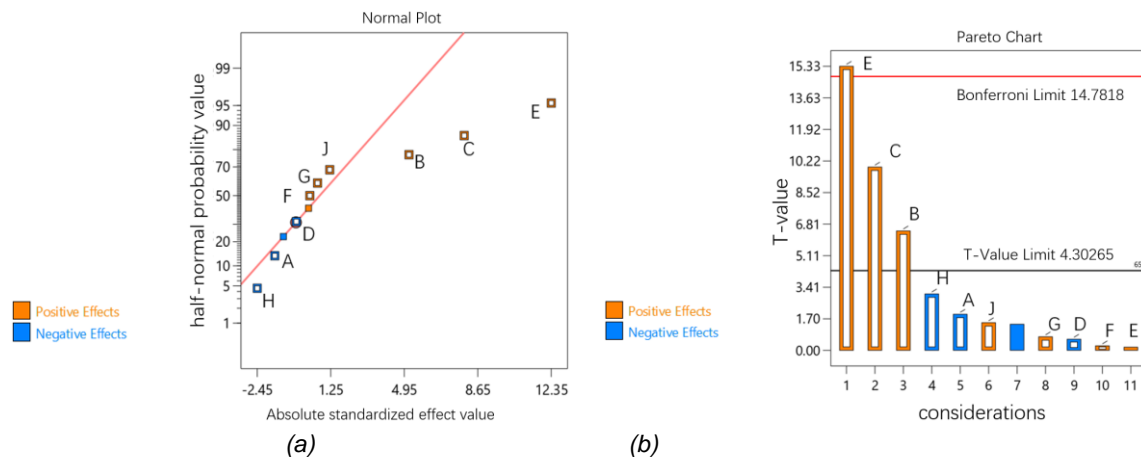


Fig. 7 - Half-normal probability effect plot for standardized effects and Pareto chart of standardization effects

A: Buckwheat Intercollision Recovery Coefficient; B: Coefficient of static friction between buckwheat seeds; C: coefficient of rolling friction between buckwheat seeds; D: Buckwheat seeds-stainless steel crash recovery coefficient; E: Buckwheat seeds-stainless steel static friction coefficient; F: Buckwheat seeds-stainless steel coefficient of kinetic friction; G: Buckwheat Poisson's ratio; H: Buckwheat density; J: Buckwheat Shear Modulus

As can be seen in Table 4, the p-value of the model is  $0.0018 < 0.05$ , which indicates significance, so the design is reliable and well fitted over the entire regression area of the study; the complex correlation coefficient  $R^2 = 0.9644$ , which indicates good correlation; and the corrected coefficient of determination  $R^2_{adj} = 0.9216$ , which indicates that 92.16% of the variability of the experimental data can be accounted for by this regression model (Dun G et al., 2024).

Table 4

Plackett-Burman test factors, levels and significant analysis

Source	Square sum	Degrees of freedom	Mean square	F-value	P-value	
mould	760.04	9	84.45	43.38	0.0227	statistically significant
A	7.36	1	7.36	3.78	0.1914	
B	80.78	1	80.78	41.50	0.0233	
C	190.36	1	190.36	97.79	0.0101	
D	0.6984	1	0.69	0.36	0.6100	
E	457.38	1	457.38	234.96	0.0042	
F	0.1151	1	0.11	0.06	0.8306	
G	1.03	1	1.03	0.53	0.5427	
H	18.00	1	18.00	9.24	0.0933	
J	4.31	1	4.31	2.22	0.2750	
Residual	3.89	2	1.95			
Aggregate	763.93	11				

Typically, a lower coefficient of variation (CV) indicates greater reliability and accuracy of the test. In this case, a CV of 10.13% suggests that the Plackett-Burman test has acceptable reliability and accuracy. Additionally, precision, defined as the ratio of effective signal to noise, is considered reasonable when it exceeds 4.0. The precision of this test is 14.5784, confirming its reliability.

● Steepest Climb Test

By fitting a multiple regression equation to the data, the regression equation was obtained:  $Y = 23.03 - 0.7829A + 2.59B + 3.98C - 0.2412D + 6.17E + 0.0979F + 0.2929G - 1.22H + 0.5996J$  (2)

From the formula, it can be seen that the partial regression coefficient of factor B is 2.59, indicating that factor B has a positive effect on the angle of repose; as factor B increases, the angle of repose will also increase. Factors C and E also exhibit positive effects.

As can be seen from Figure 7(a), the standardized effect points of factors B, C, and E are far from the fitting line, indicating that they are significant influencing factors. Furthermore, Figure 7(b) further determines the magnitude and importance of these effects, and factors B, C, and E all exceed the critical t-values as significant factors. Therefore, only these three factors are considered.

Since the most significant factor is E, E is used as the unit of climb.

Step E

$$\frac{0.7 - 0.2}{2} = 0.25 \tag{3}$$

Step C

$$\frac{3.98}{6.17} * \frac{0.1 - 0.01}{2} = 0.029 \tag{4}$$

Based on the experimental results, a value of 0.03 was utilized.

Step B

$$\frac{2.59}{6.17} * \frac{0.61 - 0.3}{2} = 0.065 \tag{5}$$

Based on the experimental results, a value of 0.07 was utilized.

The rest of the test parameters were buckwheat seeds collision recovery coefficient of 0.3, buckwheat seeds - stainless steel collision recovery coefficient of 0.5, buckwheat seeds - stainless steel coefficient of kinetic friction of 0.1, buckwheat Poisson's ratio of 0.3, buckwheat density of 1250, buckwheat shear modulus of 3.43E + 06. The results of the experimental design are shown in Table 5.

Table 5

Results of the steepest climb test design

A: Buck wheat Inter-collision Recovery Coefficient	B: Coefficient of static friction between buckwheat seeds	C: Coefficient of rolling friction between buckwheat seeds	D: Buckwheat seeds - stainless steel crash recovery coefficient	E: Buckwheat seeds - stainless steel static friction coefficient	F: Buckwheat seeds - stainless steel coefficient of kinetic friction	G: Buckwheat Poisson's ratio	H: Buckwheat density / (kg/m <sup>3</sup> )	J: Buckwheat shear modulus / Pa	Angle of repose / (°)		
0.3	0.3	0.01	0.5	0.2	0.1	0.3	1250	3.43E+06	12.41	11.4	11.91
0.3	0.37	0.04	0.5	0.45	0.1	0.3	1250	3.43E+06	27.51	27.18	27.35
0.3	0.44	0.07	0.5	0.7	0.1	0.3	1250	3.43E+06	32.49	30.58	31.54
0.3	0.51	0.1	0.5	0.95	0.1	0.3	1250	3.43E+06	38.05	36	37.02
0.3	0.58	0.13	0.5	1.2	0.1	0.3	1250	3.43E+06	41.87	41.11	41.49
0.3	0.65	0.16	0.5	0.45	0.1	0.3	1250	3.43E+06	43.05	43.69	43.37

The steepest climb test was performed to calculate the relative error between the steepest climb test rest angle β and the physical test rest angle α using the formula Y. Y=(|β-α|)/α\*100%. From the relative error, it can be seen that test 2 can be used as the centre point of the response surface test.

● Response surface methodology tests

According to the steepest climb test, the Box-Behnken test was implemented with test 2 as the centre point, and three factors of static friction coefficient between buckwheat seeds, rolling friction coefficient between buckwheat seeds and static friction coefficient between buckwheat seeds and buckwheat seeds-stainless steel were selected as the independent variables, and a three-factor, three-level test was established according to the Box-Behnken design with the angle of repose as the response value. The experimental design is shown in Table 6 (Jyoti et al., 2019; Zhang et al., 2015).

Table 6

Level	Considerations	Coefficient of static friction between buckwheat seeds	Coefficient of rolling friction between buckwheat seeds	Buckwheat seeds-stainless steel static friction coefficient
1		0.36	0.03	0.44
2		0.37	0.04	0.45
3		0.38	0.05	0.46

**RESULTS**

● **Box-Behnken test data processing**

The experimental results of the Box-Behnken test are shown in Table 7.

**Table 7**

**Box-Behnken experimental design and its results**

Test number	Coefficient of static friction between buckwheat seeds	Coefficient of rolling friction between buckwheat seeds	Buckwheat seeds-stainless steel static friction coefficient	Angle of repose / (°)
1	0.37	0.04	0.45	27.87
2	0.36	0.03	0.45	27.19
3	0.38	0.04	0.46	32.53
4	0.37	0.03	0.46	29.27
5	0.36	0.05	0.45	30.03
6	0.38	0.05	0.45	31.73
7	0.37	0.03	0.44	28.68
8	0.38	0.03	0.45	30.16
9	0.38	0.04	0.44	31.22
10	0.37	0.04	0.45	27.67
11	0.37	0.05	0.46	32.1
12	0.37	0.04	0.45	27.72
13	0.37	0.04	0.45	27.56
14	0.37	0.04	0.45	27.28
15	0.37	0.05	0.44	30.38
16	0.36	0.04	0.44	29.53
17	0.36	0.04	0.46	30.16

A quadratic polynomial equation was obtained by fitting a quadratic multiple regression to the data:

$$Y = 27.62 + 1.09A + 1.12B + 0.5313C - 0.3175AB + 0.1700AC + 0.2825BC + 1.45A^2 + 0.7025B^2 + 1.79C^2 \quad (6)$$

The multivariate correlation coefficient of the equation is R2=0.9948, which indicates that the model fits well to the actual situation, and the experimental results can be analysed by the equation, and the results of the ANOVA of the response surface test are shown in Table 8.

**Table 8**

**Box-Behnken experimental design quadratic model ANOVA**

Source	Square sum	Degrees of freedom	Mean square	F-value	P-value	
Mould	49.46	9	5.50	148.16	< 0.0001	significant
A-buckwheat static friction	9.53	1	9.53	256.86	< 0.0001	significant
B-roll friction between buckwheat	9.99	1	9.99	269.36	< 0.0001	significant
C-buckwheat-stainless steel static friction	2.26	1	2.26	60.88	0.0001	significant
AB	0.4032	1	0.4032	10.87	0.0132	significant
AC	0.1156	1	0.1156	3.12	0.1208	
BC	0.3192	1	0.3192	8.61	0.0219	significant

Source	Square sum	Degrees of freedom	Mean square	F-value	P-value	
A <sup>2</sup>	8.91	1	8.91	240.33	< 0.0001	significant
B <sup>2</sup>	2.08	1	2.08	56.02	0.0001	significant
C <sup>2</sup>	13.42	1	13.42	361.71	< 0.0001	significant
residual	0.2596	7	0.0371			
incoherent	0.0654	3	0.0218	0.4492	0.7316	insignificant
inaccuracies	0.1942	4	0.0485			
CV (%)	0.6534					
			R2	0.9948	R2adj	0.9881

As can be seen from Table 8, the model is highly significant ( $P < 0.05$ ) while the out-of-fit term is not significant ( $P > 0.05$ ), the model correlation coefficient  $R^2 = 0.9948$  and the correction coefficient  $R^2_{adj} = 0.9881$ , which indicates that the model fit is better, and the model can explain 98.81% of the variation of the response value, and the angle of repose can be analysed and predicted using this model. From the results in Table 8, it can be seen that the factors primary terms A, B and C have significant effect on the angle of repose; the interaction terms AB, BC have significant effect on the angle of repose and AC has insignificant effect; the secondary terms A<sup>2</sup>, B<sup>2</sup>, C<sup>2</sup> have significant effect on the angle of repose. This indicates that the relationship between the factors and the response value is not a simple linear relationship, the degree of influence of the factors is:  $B > A > C$ , i.e., rolling friction between buckwheat seeds > static friction between buckwheat seeds > buckwheat seeds - stainless steel static friction.

The angle of repose was predicted using the regression model, and in order to facilitate the observation of the model prediction results, the correlation graph between the model predicted values and the experimental values was plotted. From Fig. 8, it can be found that the sample points are all in the vicinity of the 45° diagonal, indicating that the model's prediction of the angle of repose under each factor is highly correlated with the experimental values, and the difference between the two is relatively small. Figure 9 illustrates the distribution of the model's prediction error. A reliable model typically requires that the prediction error for most samples remains within the  $\pm 2SD$  range.

As shown in Figure 9, all sample points lie within this range, with no anomalies observed. This indicates that the model has high prediction accuracy and is suitable for analysing the angle of repose.

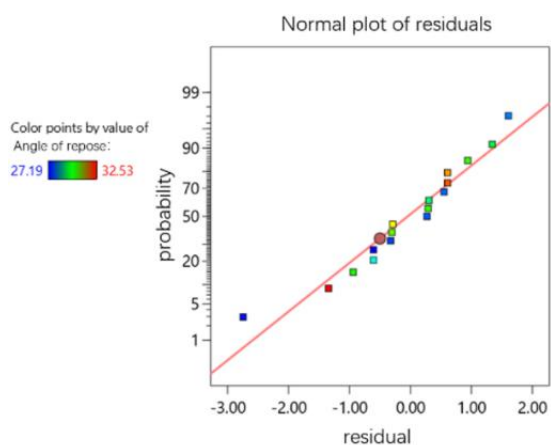


Fig. 8 - Correlation of model predicted values with experimental values

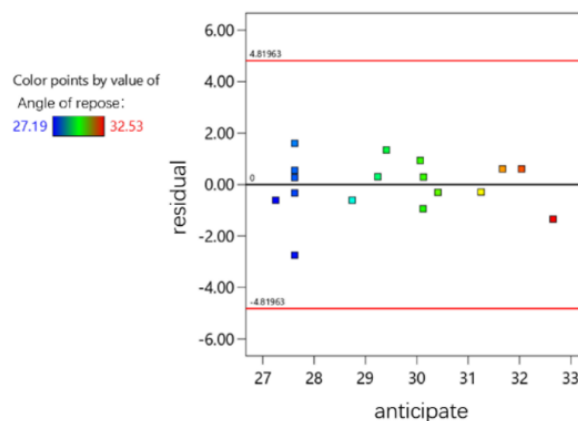


Fig. 9 - Plot of residuals on model predicted walks

Based on the regression equation, the response surface analysis was plotted using Design-expert and the results are shown in Figure 10. The three-dimensional plot of the response surface can be clearly seen through the range of tests performed including the area where the minimum value is located.

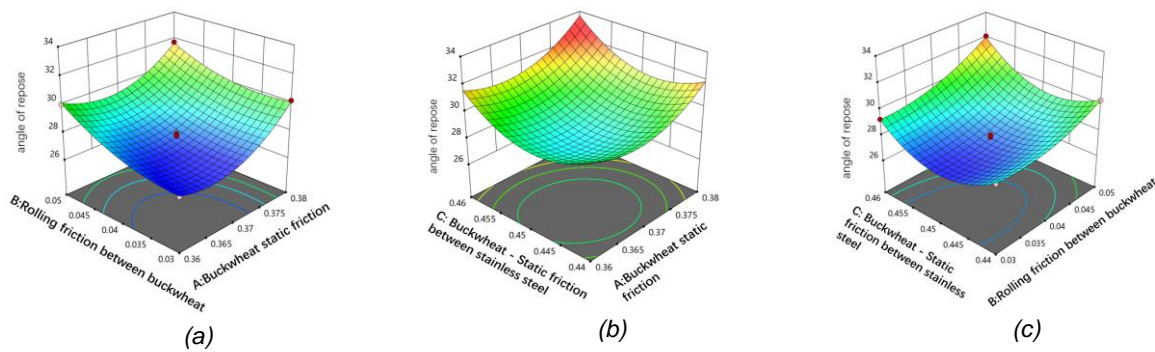


Fig. 10 - Response surface analysis plot

Response surface analysis plotted using Design-expert shows that static friction between buckwheat seeds and rolling friction interaction between buckwheat seeds-stainless steel have a significant effect on the angle of repose.

#### ● Determination of optimal combination parameters and validation results

Based on the optimization module in the Design-Expert software, the regression model was optimized and solved with the target value of  $27.65^\circ$  of the physical test, and parameters similar to those of the physical test were obtained: the coefficient of static friction between buckwheat seeds was 0.372, the coefficient of rolling friction between buckwheat seeds was 0.038, and the coefficient of static friction between buckwheat seeds-stainless steel was: 0.448.

#### CONCLUSIONS

(1) A simulation model for the stacking angle of repose of buckwheat seeds was developed using EDEM software. MATLAB image processing technology was employed to linearly fit the edge contour of the angle of repose, providing an accurate response value. The results of the Plackett-Burman test indicate that the static friction coefficient between buckwheat seeds, the rolling friction coefficient between buckwheat seeds, and the static friction coefficient between buckwheat seeds and stainless steel significantly influence the angle of repose;

(2) Based on the results of the Box-Behnken response surface test, a quadratic regression model was developed to describe the relationship between significant parameters and the angle of repose. The analysis of variance revealed that the primary terms (static friction coefficient between buckwheat seeds, rolling friction coefficient between buckwheat seeds, and static friction coefficient between buckwheat seeds and stainless steel), the interaction terms (static friction coefficient and rolling friction coefficient between buckwheat seeds, as well as rolling friction coefficient and static friction coefficient between buckwheat seeds and stainless steel), and the quadratic terms of these coefficients significantly affect the angle of repose.

(3) By optimizing the regression equation to find the optimal solution, the following values were obtained: a static friction coefficient of 0.372 for buckwheat, a rolling friction coefficient of 0.038 for buckwheat, and a static friction coefficient of 0.448 for the buckwheat-stainless steel interaction. The remaining parameters were set to their intermediate levels. The relative error between the physical test results and the simulation outcomes was 1.08%, indicating that the contact parameters and the contact model parameters are both accurate and reliable.

#### ACKNOWLEDGEMENT

This research was funded by the Shanxi Province Basic Research Program (No.202203021212417). Shanxi Agricultural University Academic Restoration Project (No.2023XSHF2). Central guidance for local scientific and technological development funding projects (No. YDZJSX20231C009);

#### REFERENCES

- [1] Chen G. (2024). Parameter calibration and experiment of discrete element simulation of spherical-like soybean based on DEM. (基于 DEM 的类球型大豆离散元仿真参数标定与试验). *INMATEH - Agricultural Engineering*, Vol.74, Issue 03, pp.303-315.

- [2] Dun G. (2024). Simulation of soybean seed physical properties on filling performance (大豆种子物理特性对充种性能影响的仿真研究). *INMATEH - Agricultural Engineering*, Vol.74, Issue 03, pp.95-104.
- [3] González-Montellano, C, (2012). Determination of the mechanical properties of maize grains and olives required for use in DEM simulations. *Journal of Food Engineering*, Vol.111, Issue 4, pp. 553-562.
- [4] Jyoti G. (2019). Optimization of esterification of acrylic acid and ethanol by Box-Behnken design of response surface methodology. *Indian Journal of Chemical Technology*, Vol. 26, Issue 1, pp. 89-94;
- [5] Lei X. (2023). Determination of Material and Interaction Properties of Granular Fertilizer Particles Using DEM Simulation and Bench Testing. *Agriculture*, Vol.13, Issue 9, pp. 1704;
- [6] Li Y.X. (2019). Discrete meta-parameter calibration of wheat flour based on particle scaling (基于颗粒缩放的小麦粉离散元参数标定). *Journal of Agricultural Engineering*, Vol.35, Issue 16, pp. 320-327;
- [7] Li G. (2023). Establishment and Calibration of Discrete Element Model for Buckwheat Seed Based on Static and Dynamic Verification Test. *Agriculture*, Vol.13, Issue 5;
- [8] Liu W.Z. (2018). Parameter calibration for micro potato simulation based on discrete elements (基于离散元的微型马铃薯仿真参数标定). *Journal of Agricultural Machinery*, Vol.49, Issue 05, pp. 125-135+142;
- [9] Rittisak S. (2023). Application of the Plackett-Burman design for screening and optimisation of factors affecting the aqueous extract for total anthocyanin content of broken riceberry rice. *International Food Research Journal*, Vol.30, Issue 3, pp. 649-655;
- [10] Wang C J, (2012). Determination of the coefficient of recovery in a wheat grain collision model (小麦籽粒碰撞模型中恢复系数的测定). *Journal of Agricultural Engineering*, Vol.28, Issue 11, pp. 274-278, Huainan / P.R.C.;
- [11] Wu J.S. (2019). Determination of Physical Properties of Qianhu Seeds and Calibration of Parameters of Discrete Element Simulation Model (前胡种子物性参数测定及其离散元仿真模型参数标定). *Journal of Gansu Agricultural University*, Vol.54, Issue 04, pp. 180-189;
- [12] Wu L.G. (2018). Buckwheat Nutritional and Functional Properties and Related Food Development Research Progress (荞麦营养功能特性及相关食品开发研究进展). *Grain, Oil and Food Science and Technology*, Vol.26, Issue 03, pp. 41-44;
- [13] Xu B. (2021). Construction of a discrete element model of buckwheat grain and calibration of parameters. *INMATEH - Agricultural Engineering*, Vol 64, Issue 2 , pp. 175-184;
- [14] Xu T. (2023). Ellipsoidal seed modeling and simulation parameter selection based on the discrete element method. *Materials Today Communications*, Vol. 37;
- [15] Zeng Z.W. (2021). Current status and perspectives of the application of discrete element method in agricultural engineering research (离散元法在农业工程研究中的应用现状和展望). *Journal of Agricultural Machinery*, Vol.52, Issue 04, pp. 1-20.
- [16] Zhang R, (2017). Research on calibration method of sand parameters in discrete element simulation (离散元模拟中沙土参数标定方法研究). *Journal of Agricultural Machinery*, Vol.48, Issue 03, pp. 49-56;
- [17] Zhang Y-j. (2015). Optimization of one-step pelletization technology of Biqu granules by Plackett-Burman design and Box-Behnken response surface methodology. *China journal of Chinese materia medica*, Vol.40, Issue 22, pp. 4406-4410.